PHYSICAL REVIEW LETTERS

Proposed Measurement of Spatial Correlations at the Berezinski-Kosterlitz-Thouless Transition of Superconducting Thin Films

Amir Erez and Yigal Meir

Physics Department, Ben-Gurion University of the Negev, Beer Sheva 84105, Israel

The Berezinski-Kosterlitz-Thouless transition is a unique two-dimensional phase transition, separating two phases with exponentially and power-law decaying correlations, respectively. In disordered systems, these correlations propagate along favorable paths, with the transition marking the point where global coherence is lost. Here we propose an experimental method to probe locally these particular paths in superconducting thin films, which exhibit this transition, and demonstrate theoretically that close to the transition the coherence propagates along a ramified network, reminiscent of a percolation transition. We suggest and calculate experimentally accessible quantities that can shed light on the spatial correlations in the system as it approaches the critical point. This approach can be applicable to a variety of phase transitions in disordered systems.

According to the Mermin-Wagner theorem [1] there can be no long-range order (of continuous symmetry) at any finite temperature in two-dimensional systems. Nevertheless, one may expect a finite-temperature Berezinski-Kosterlitz–Thouless (BKT) transition [2–4] between a phase with power-law decaying correlations at $T < T_{BKT}$ and a phase with exponentially decaying correlations at $T > T_{BKT}$. This BKT transition is driven by the unbinding and proliferation of vortex-antivortex pairs at the critical temperature T_{BKT}, which destroy global phase coherence. It was suggested [5] that such a BKT transition can be realized as a superconductor-insulator transition in thin disordered films, where one of the hallmarks of the BKT transition is a universal jump in the superfluid stiffness [6] at the critical temperature. This superconductor-insulator transition in thin films has been the subject of intense experimental and theoretical research for several decades [7], yet many puzzles remain.

In such disordered films, it has been established theoretically [8–13] and observed experimentally [14–17] that the superconducting (SC) order parameter fluctuates strongly across the sample, creating "SC islands," where the SC order is high, surrounded by areas of weaker SC correlations. With increasing temperature the coherence between neighboring SC islands is suppressed, until percolation of coherence from one side of the sample to the other is lost, leading to the loss of global SC order [12,13,18,19]. This description predicts that local SC order may persist even when global SC order is lost, consistent with experiments [20–26].

It has not been established whether the above process is an alternative description of the BKT transition in a disordered system or describes a different phase transition. The Harris criterion [27] indicates that the BKT transition is stable under weak disorder, and recent experimental [28] and theoretical [13] studies on disordered superconductors

demonstrated the consistency of the transition in disordered systems with BKT physics (see, however, Ref. [29]). The latter calculation also showed that the BKT transition is indeed concomitant with percolation of near-neighbor correlations.

Understanding how coherence propagates in such disordered systems is thus crucial to resolving the nature of the transition. In this Letter, we propose an experimental procedure based on an established experimental technique [30–32], whereby the change in a global quantity, such as the resistance or the superfluid response, is measured as a function of a local perturbation, such as a charged AFM or STM tip, which can be scanned across the system. A significant change in the conductance, for example, indicates that the area under the tip carries, in the absence of the tip, a significant portion of the current through the sample, while small changes indicate areas the current tends to avoid. Such a procedure produced clear maps of the modes of transport in quantum point contacts [30,32] and in the quantum Hall regime [31]. Generalizing the same procedure to SC thin films will allow spatial resolution of the local propagation of coherence in disordered superconductors, and, more generally, in disordered systems manifesting the BKT transition. (Standard scanning STM measurements have already been done in thin SC films by, e.g., Refs. [16,17].) Here we produce numerical simulations of the experimental procedure on a square lattice, and make specific predictions. A main result of our work is that indeed certain links carry more of the global coherence as the critical temperature T_{BKT} is approached and that these links form a ramified network. We then present further evidence supporting the percolation hypothesis by showing a connection between this network and the Wolff cluster [33], which is known to percolate at T_{BKT} [34]. As we demonstrate, the measurement will allow a direct probe of local and long-range

correlations in the system, which will provide a detailed description of the transition. We expect our approach to be directly generalizable to other phase transitions in disordered systems.

Model and method.—A minimal model that captures the BKT behavior in two dimensions is the classical *XY* model. It neglects the fermionic excitations possible when Cooper pairs are broken into two quasiparticles, yet it captures the loss of global phase coherence by a BKT transition. This model is relevant to low-dimensional superconductors [5], where loss of phase coherence dictates the transition temperature T_{BKT}, which is much lower than the SC gap, the quasiparticle excitation energy [35,36].

The model is described by the Hamiltonian

$$\mathcal{H}_{\mathrm{XY}} = -\sum_{\langle ij \rangle} J_{ij} \cos(\theta_i - \theta_j) \qquad (1)$$

with $\theta_i \in [0, 2\pi]$ an angle in the *XY* plane; $\langle ij \rangle$ denotes nearest neighbors. J_{ij}, the random nearest neighbor couplings, are taken from a log-box distribution $J_{ij} = J_0 \exp(x)$ with x distributed uniformly between $-\lambda$ and $+\lambda$, and $\lambda \geq 0$ thus controls the disorder strength (such a distribution is naturally expected in disordered thin films, where the Josephson coupling is exponential in the distance between the superconducting area). The distribution is chosen such that the median value of J_{ij} is J_0, defined as the unit of energy, regardless of the disorder λ. In what follows we present results for $\lambda = 5$, which provides values of J_{ij} over many orders of magnitude while still allowing enough numerical accuracy, but we find similar results for a range of λ. We simulate the model using the classical Monte Carlo Wolff algorithm [33] with periodic boundary conditions in both directions.

The global quantity that we study is the superfluid response, or the helicity modulus. The helicity modulus Υ_x in the *x* direction is the response of the free energy F to a phase twist Φ_x in that direction and is given by the expression

$$N_x \Upsilon_x \equiv \frac{\partial^2 F}{\partial \Phi_x^2}$$
$$= \left\langle \sum_{\langle ij \rangle \| \vec{e}_x} J_{ij} \cos(\theta_{ij}) \right\rangle - \beta \left\langle \left(\sum_{\langle ij \rangle \| \vec{e}_x} J_{ij} \sin(\theta_{ij}) \right)^2 \right\rangle, \quad (2)$$

where the sums are over all bonds in the *x* direction and N_x is the number of such bonds. $\theta_{ij} = \theta_i - \theta_j$ is the phase difference between neighboring sites i, j and the large brackets denote thermal averages. Υ_y is defined similarly for a twist in the *y* direction, and we define $\Upsilon \equiv (\Upsilon_x + \Upsilon_y)/2$. At low temperatures, where phase fluctuations are suppressed, $\cos(\theta_{ij}) \approx 1 - \frac{1}{2}\theta_{ij}^2$, and the *XY* model is equivalent to a random resistor network. Since the resistance of such a network with an exponential distribution of resistances is given by the percolating

resistance [37,38], which, for the square lattice, is the median of the distribution, we expect that $\Upsilon(T)$ will be unaffected by disorder (the value of λ) for the log-box distributions studied in this work, for low temperatures. Indeed we find that $\Upsilon(T)$ is unmodified by λ at very low temperatures ($T \ll \min[J_{ij}]$) and that T_{BKT} is reduced by less than 10% for large disorder ($\lambda = 5$). Moreover, the shape of $\Upsilon(T)$ is consistent with the BKT behavior; i.e., as the system size increases, the (negative) slope in $\Upsilon(T)$ increases for $T > T_{\mathrm{BKT}}$ but not for $T < T_{\mathrm{BKT}}$, indicating a finite jump in the large size limit.

We simulate a local disturbance (such as the STM tip in the experiment) by cutting a single bond (i.e., setting a single $J_{ij} = 0$) and then measuring the resulting change in Υ, which we label $\delta\Upsilon_{ij}$. This procedure is repeated for all bonds in the lattice. Removing a bond $\{i, j\}$ in the *x* direction results in a change in the global helicity modulus

$$\delta\Upsilon_{ij} = J_{ij}\langle\cos(\theta_{ij})\rangle + \beta J_{ij}^2 \langle\sin^2(\theta_{ij})\rangle$$
$$- 2\beta J_{ij} \sum_{\langle lm \rangle \| \vec{e}_x} J_{lm}\langle\sin(\theta_{ij})\sin(\theta_{lm})\rangle, \quad (3)$$

and similarly for a bond in the *y* direction. As we are interested in linear response, the brackets here denote thermal averages with respect to the unperturbed Hamiltonian in Eq. (1) [39].

Results.—Figure 1 shows a two-dimensional map of $\delta\Upsilon_{ij}$ for a typical realization of disorder at $\lambda = 5$ for a 128×128 periodic lattice, at two temperatures $T \ll T_{\mathrm{BKT}}$ and $T \approx T_{\mathrm{BKT}}$. (To display the bond values, we map each bond to a site using the established technique of a covering lattice [40].) Darker bonds mark those bonds that when cut make a stronger change to the helicity modulus. For $T \ll T_{\mathrm{BKT}}$ [see Fig. 1(a)] it is evident that the bonds that contribute significantly to global coherence form a dense network. As T approaches T_{BKT} [see Fig. 1(b)], these bonds form a very ramified network, consisting of distinct channels, even though the disorder does not have any spatial correlations. In Fig. 1(c) we plot the spatial histogram of the values of $\delta\Upsilon(T)/\Upsilon(T)$ for a range of temperatures. Three features in the histogram are noteworthy. (i) The median of $\delta\Upsilon/\Upsilon$ does not change with temperature. (ii) As temperature is increased towards T_{BKT}, the peak of the distribution (the range of $\delta\Upsilon/\Upsilon$ between the arrows) gets suppressed and the weight is shifted to the tails of very strong and very weak $\delta\Upsilon$ values. (iii) The distribution is a sum of two peaked distributions, one centered around high $\delta\Upsilon$ (near the right arrow) and one around small values (left arrow). The two broken lines denote the distributions of $\delta\Upsilon/\Upsilon$ generated by the bonds with a microscopic $J_{ij} < 1$ (left) and those with $J_{ij} > 1$ (right), revealing a correlation between $\delta\Upsilon$ and J_{ij} (see below). As disorder (λ) is increased, the peaks grow farther apart.

Consequently, the following physical picture emerges: at low temperature the sample is mostly coherent and there
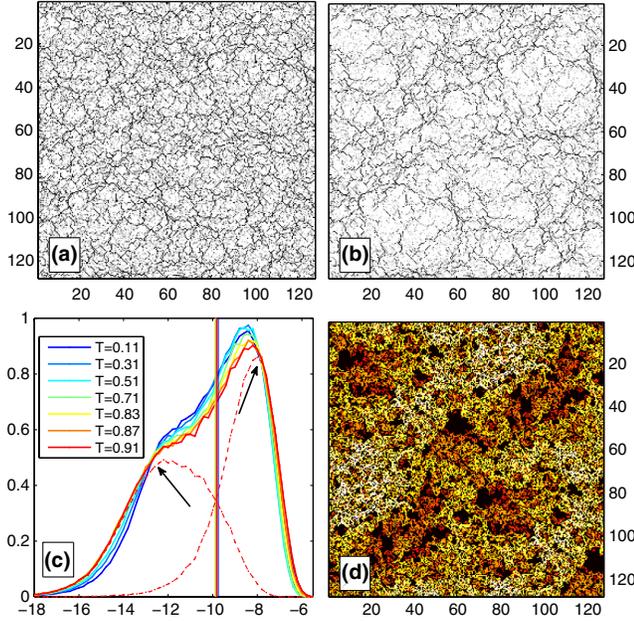
FIG. 1 (color online). δY for a typical realization of disorder at $\lambda = 5$ for a 128×128 periodic lattice, for $T = 0.11 \ll T_{\mathrm{BKT}}$ (a) and $T = 0.89 \approx T_{\mathrm{BKT}}$ (b). As temperature increases towards T_{BKT}, coherence propagates through specific channels, forming a ramified network. (c) The distribution $P(\delta Y / Y)$ at $T = 0.11$–0.91 showing a constant median (vertical lines) and a shift of the weight to the tails with increasing temperatures (change points marked by the arrows). Broken lines: the distribution at $T = 0.89$ divided to the $J < 1$ (left) and $J > 1$ (right) components. (d) P_w (probability to belong to a Wolff cluster) at $T = 0.89$ showing the same spatial structure of the Wolff clusters as the δY plot in (b).

are many routes for the global phase coherence to propagate through the sample; thus, many bonds give a significant contribution when cut. As temperature increases towards T_{BKT}, larger regions lose coherence, so the coherent routes gradually thin out, limiting the propagation of global coherence to a smaller set of bonds, forming a ramified network of channels.

Naively, one might suspect that there exists a trivial relation between the bare microscopic couplings J_{ij} and their global effect δY_{ij}, as might be inferred from Eq. (3). Yet Fig. 2(a) reveals a more interesting relation: for submedian bonds $J_{ij} < 1$, there is a linear correlation $\delta Y_{ij} \propto J_{ij}$ as suggested by the unit slope of the log plot. However, for half the bonds of the lattice, for which $J_{ij} > 1$, δY_{ij} is only weakly dependent on J_{ij} (the exact relation depends on λ). The reason is that these bonds belong to the percolating coherence cluster, and the effect of cutting such a bond on δY_{ij} depends no longer only on its bare coupling J_{ij} but rather on its location in the network. We consider this behavior and its onset at the median bond (which is the percolation threshold for the square lattice) as further evidence supporting the percolation scenario.
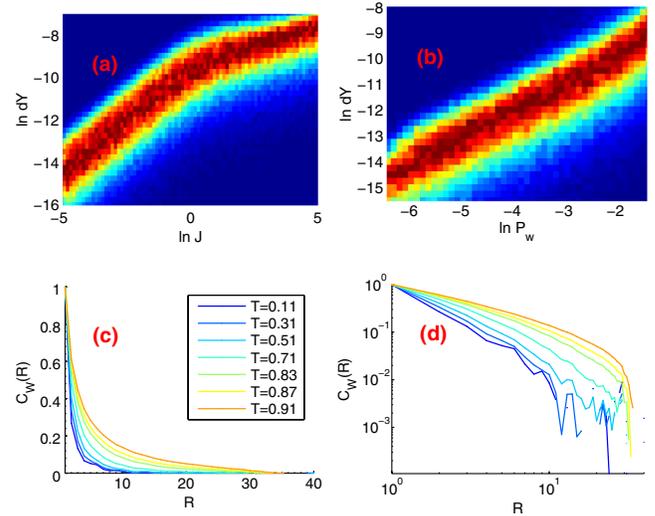
FIG. 2 (color online).   (a) Normalized scatter plot of $\ln \delta Y$ vs $\ln J$ showing correlation only for the submedian bonds ($\ln J < 0$). (b) Normalized scatter plot of $\ln \delta Y$ vs $\ln P_w$ (probability to belong to a Wolff cluster) showing a clear linear correlation. $C_W(R)$, the correlation function for P_w, for a range of temperatures on a (c) linear and (d) log-log scale. The correlation decays more slowly at higher temperatures, indicating the sparsity of the coherence propagation.

In order to shed more light upon the spatial structure of the correlation, we turn our attention to the Wolff clusters [33]. *A priori*, these are mere numerical constructs that were introduced to overcome the numerical problem within the Metropolis Monte Carlo algorithm, which is based on updates of local variables (such as spins), depending on Boltzmann weights. Because of the divergence of length scales near the transition, spins are highly correlated on large scales, and single spin flips are highly improbable. To address this problem Wolff [33] proposed a very efficient algorithm, which eliminated this critical slowing down by allowing clusters of spins, called Wolff clusters, to flip together. These clusters are constructed stochastically according to near-neighbor correlations. It was later suggested [41] and then proven rigorously [34] that the efficiency of the algorithm lies in its correct capture of the physics of the BKT transition. The size of the Wolff clusters, which reflect the correlated spins, grows towards the BKT transition, the latter happening exactly where the Wolff cluster percolates through the whole system. Note that this proof applies for a clean system—the random structure of the Wolff cluster is a result of the stochastic nature of its construction, so one can imagine that they reflect the random temporal correlations of the spins. Nevertheless, due to the uniformity of the system, the probability of every bond $\langle ij \rangle$ to belong to a Wolff cluster P_{ij}^W is the same. This situation is very different in disordered systems. The Wolff clusters, generated during the Monte Carlo calculation, are highly anisotropic and reflect the spatial disorder in the system. In Fig. 1(d) we display a

two-dimensional plot of the probability P_{ij}^w at $T \approx T_{\text{BKT}}$. Indeed, P_{ij}^w and $\delta\Upsilon$ [see Fig. 1(b)] exhibit very similar spatial structure, so the bonds with high $\delta\Upsilon$, darkest in Fig. 1(b), are also the ones with the highest probability to be part of a Wolff cluster, brightest in Fig. 1(d). Hence the bonds that support the propagation of coherence (i.e., have a large $\delta\Upsilon$) are also, as expected, the ones that have long-range correlations, as reflected by the Wolff clusters. This observation is further supported by Fig. 2(b), which displays a normalized scatter plot of $\delta\Upsilon_{ij}$ vs P_{ij}^w, demonstrating the clear correlation between over 10 orders of magnitude. If the proof that the Wolff clusters percolate at the BKT transition extends to the disordered case, as is indicated numerically, it is yet further support for the percolating nature of coherence at the BKT transition.

A further check on the changing spatial structure with temperature can be revealed by studying the correlation function

$$C_\Upsilon(R) \equiv \frac{\sum_{|\langle ij\rangle - \langle kl\rangle| = R}(\delta\Upsilon_{ij} - \overline{\delta\Upsilon})(\delta\Upsilon_{kl} - \overline{\delta\Upsilon})}{\sum_{|\langle ij\rangle - \langle kl\rangle| = R}}, \quad (4)$$

where the sum is over all pairs of bonds, a distance R apart, and $\overline{\delta\Upsilon}$ is the asymptotic average of $\delta\Upsilon_{ij}$, so that $C_Y(R)$ decays to zero at large R. A similar correlation function $C_W(R)$ can be defined in terms of P_{ij}^w. Because of the high correlations between P_{ij}^w and $\delta\Upsilon_{ij}$ [see Fig. 2(b)] we find a similar behavior for these two correlation functions, though $C_W(R)$ displays smaller statistical fluctuations. Figure 2(c) depicts $C_W(R)$ at a range of temperatures and Fig. 2(d) depicts it on a log-log scale. At low temperatures, as the network supporting coherence is dense, $C_W(R)$ decays quickly to zero. As temperature increases there is a marked slower decay of $C_W(R)$, demonstrating the ramified nature of that network. For the system sizes we simulated, the correlation function doesn't follow any simple decay law, possibly due to finite size effects.

Summary and discussion.—The effect of disorder on the BKT transition is a hotly debated problem in condensed matter physics, and its relation to percolation, or the emergence of a new critical point, are open issues. In this Letter we propose an experiment to probe the spatial structure of global phase coherence in two-dimensional superconductors, which are expected to display such a transition. Our proposition is based on similar experiments that probe conductance channels through quantum point contacts and in quantum hall systems (while, for theoretical convenience, we display results for the phase stiffness, we expect similar results for the current). We present numerical results for a minimal model that (in its clean version) displays a BKT transition, in the strong disorder regime. Our numerics point at an intriguing mechanism where the global coherence passes predominantly through specific channels that can be experimentally probed. The correlation functions we have calculated, which can also be

measured experimentally, also support the idea that as the critical temperature is approached, the coherence network becomes more ramified, with percolation lost at T_{BKT}. This picture is further supported theoretically by the robust correlation between these channels and the structure of the Wolff clusters, objects known to percolate at the phase coherence transition of clean systems. Moreover, our tests at $\lambda > 5$ show that the two peaks [broken lines in Fig. 1(c)] move apart as disorder increases. This suggests the tempting possibility that at large enough λ the two peaks separate out and can thus give the experimentalist a clear map of where coherence propagates, in addition to a direct determination of which of the local Josephson couplings are below the median as opposed to above the median. It is interesting to note that as temperature increases towards T_{BKT}, a significant fraction (up to approximately 40%) of the $\delta\Upsilon$ values become negative, indicating an increase in coherence when these bonds are cut. Such behavior is certainly possible in coherent systems, but is a departure from known results on random resistor networks [42,43], which is relevant to the XY model at low temperatures. Again, this observation is consistent with the percolation pictures: cutting links that do not participate in the network that support the propagation of coherence not only does not impede the global coherence, but may, in fact, increase it by giving more weight to the percolating network. The experiment suggested here and the numerical method can, in fact, be applied to any physical system involving a phase transition driven by phase fluctuations, and may also be relevant to high-T_C superconductors in part of their phase diagram [35].

The method suggested and analyzed in this Letter can, in fact, be used to probe the spatial correlations in other phase transitions in disordered systems, and to shed light on the intriguing interplay between disorder and correlations in such systems.

[1] N. D. Mermin and H. Wagner, Phys. Rev. Lett. **17**, 1133 (1966).
[2] V. L. Berezinski, J. Exp. Theor. Phys. **34**, 610 (1972).
[3] J. M. Kosterlitz and D. J. Thouless, J. Phys. C **6**, 1181 (1973).
[4] J. M. Kosterlitz, J. Phys. C **7**, 1046 (1974).
[5] M. R. Beasley, J. E. Mooij, and T. P. Orlando, Phys. Rev. Lett. **42**, 1165 (1979).
[6] M. E. Fisher, M. N. Barber, and D. Jasnow, Phys. Rev. A **8**, 1111 (1973).
[7] A. M. Goldman, Int. J. Mod. Phys. B **24**, 4081 (2010).
[8] B. Spivak and F. Zhou, Phys. Rev. Lett. **74**, 2800 (1995).
[9] F. Zhou and B. Spivak, Phys. Rev. Lett. **80**, 5647 (1998).

[10] V. M. Galitski and A. I. Larkin, Phys. Rev. Lett. **87,** 087001 (2001).

[11] A. Ghosal, M. Randeria, and N. Trivedi, Phys. Rev. B **65,** 014501 (2001).

[12] Y. Dubi, Y. Meir, and Y. Avishai, Nature (London) **449,** 876 (2007).

[13] A. Erez and Y. Meir, Europhys. Lett. **91,** 47003 (2010).

[14] D. Kowal and Z. Ovadyahu, Solid State Commun. **90,** 783 (1994).

[15] C. Howald, P. Fournier, and A. Kapitulnik, Phys. Rev. B **64,** 100504 (2001).

[16] B. Sacepe, C. Chapelier, T. I. Baturina, V. M. Vinokur, M. R. Baklanov, and M. Sanquer, Phys. Rev. Lett. **101,** 157006 (2008).

[17] B. Sacepe, T. Dubouchet, C. Chapelier, M. Sanquer, M. Ovadia, D. Shahar, M. Feigelman, and L. Ioffe, Nat. Phys. **7,** 239 (2011).

[18] R. T. Scalettar, N. Trivedi, and C. Huscroft, Phys. Rev. B **59,** 4364 (1999).

[19] G. Seibold, L. Benfatto, C. Castellani, and J. Lorenzana, Phys. Rev. Lett. **108,** 207004 (2012).

[20] A. Yazdani and A. Kapitulnik, Phys. Rev. Lett. **74,** 3037 (1995).

[21] V. Gantmakher, M. Golubkov, V. Dolgopolov, G. Tsydynzhapov, and A. Shashkin, JETP Lett. **68,** 363 (1998).

[22] R. Crane, N. P. Armitage, A. Johansson, G. Sambandamurthy, D. Shahar, and G. Gruner, Phys. Rev. B **75,** 184530 (2007).

[23] M. D. Stewart, A. Yin, J. M. Xu, and J. M. Valles, Science **318,** 1273 (2007).

[24] M. D. Stewart, Jr., A. Yin, J. M. Xu, and J. M. Valles, Jr., Phys. Rev. B **77,** 140501 (2008).

[25] H. Q. Nguyen, S. M. Hollen, M. D. Stewart, Jr., J. Shainline, A. Yin, J. M. Xu, and J. M. Valles, Jr., Phys. Rev. Lett. **103,** 157001 (2009).

[26] W. Liu, M. Kim, G. Sambandamurthy, and N. P. Armitage, Phys. Rev. B **84,** 024511 (2011).

[27] A. B. Harris, J. Phys. C **7** 1671 (1974).

[28] S. Misra, L. Urban, M. Kim, G. Sambandamurthy, and A. Yazdani, Phys. Rev. Lett. **110,** 037002 (2013).

[29] L. Benfatto, C. Castellani, and T. Giamarchi, Phys. Rev. Lett. **98,** 117008 (2007).

[30] M. A. Topinka, B. J. LeRoy, R. M. Westervelt, S. E. J. Shaw, R. Fleischmann, E. J. Heller, K. D. Maranowski, and A. C. Gossard, Nature (London) **410,** 183 (2001).

[31] S. Kičin, A. Pioda, T. Ihn, K. Ensslin, D. C. Driscoll, and A. C. Gossard, Phys. Rev. B **70,** 205302 (2004).

[32] M. P. Jura, M. A. Topinka, L. Urban, A. Yazdani, H. Shtrikman, L. N. Pfeiffer, K. W. West, and D. Goldhaber-Gordon, Nat. Phys. **3,** 841 (2007).

[33] U. Wolff, Phys. Rev. Lett. **62,** 361 (1989).

[34] L. Chayes, Commun. Math. Phys. **197,** 623 (1998), 10.1007/s002200050466.

[35] V. J. Emery and S. A. Kivelson, Nature (London) **374,** 434 (1995).

[36] E. Carlson, V. Emery, S. Kivelson, and D. Orgad, in *Superconductivity,* edited by K. Bennemann and J. Ketterson (Springer-Verlag, Berlin, 2008), pp. 1225–1348.

[37] V. Ambegaokar, B. I. Halperin, and J. S. Langer, Phys. Rev. B **4,** 2612 (1971).

[38] P. Le Doussal, Phys. Rev. B **39,** 881 (1989).

[39] Comparison with averages with respect to the perturbed Hamiltonian shows no significant difference. See the Supplemental Material at http://link.aps.org/supplemental/10.1103/PhysRevLett.111.187002 for such a comparison.

[40] M. E. Fisher, J. Math. Phys. (N.Y.) **2,** 620 (1961).

[41] P. W. Leung and C. L. Henley, Phys. Rev. B **43,** 752 (1991).

[42] L. de Arcangelis, S. Redner, and A. Coniglio, Phys. Rev. B **31,** 4725 (1985).

[43] S. Roux, P. Rigord, A. Hansen, and E. L. Hinrichsen, Phys. Rev. B **43,** 10984 (1991).